DOI: 10.1002/ejic.200701220

Iron and Cobalt Complexes of 4-Alkyl-2,6-diiminopyridine Ligands: Synthesis and Ethylene Polymerization Catalysis

Juan Cámpora,*[a] A. Marcos Naz,[a] Pilar Palma,[a] Antonio Rodríguez-Delgado,[a] Eleuterio Álvarez,[a] Incoronata Tritto,[b] and Laura Boggioni[b]

Keywords: Iron / Cobalt / Diiminopyridine ligands / Ethylene Polymerization / Self-immobilization

A new methodology for selective alkylation of the 2,6-diiminopyridine (pdi) ligands allows the ready synthesis of new derivatives displaying 2-methyl-2-phenylpropyl (neophyl), benzyl, or allyl groups in the 4-position of the pyridine ring. A set of Fe and Co complexes containing the new ligands have been synthesized and fully characterized. The presence of 4-neophyl or -benzyl groups does not perturb the performance of the complexes as ethylene polymerization catalysts, but the introduction of the 4-allyl group leads to the production of higher molecular weight polymers.

Introduction

Since their discovery in the late 1990s,[1] iron and cobalt olefin polymerization catalysts containing 2,6-diiminopyridine (pdi) ligands have been the subject of much interest.[2] Much effort has been devoted to the modification of the ligand structure, in order to gain control of catalyst activity and polymer properties. The ligand has also been modified to provide attachment points for catalyst immobilization.[3] A large part of that work has concentrated on the systematic variation of the nitrogen aryl substituents, since these have a deep influence on the catalyst performance. Many *N*-aryl[4] and *N*-heteroaryl[5] groups displaying different substitution patterns have been investigated. Substitution at the α-imine position is another modification strategy, and not only the well-known 2,6-bis(formaldimino)pyridine and 2,6-bis(acetaldimino)pyridine ligands but a number of ligands that display different types of α-alkyl and aryl groups[6] as well as heteroatom-based functionalities (OR, SR, etc)[7] have been prepared and studied. These structural modifications of the pdi framework provide access to a wide variety of polyethylene materials and are usually based on relatively straightforward methodologies. This constitutes one of the most attractive qualities of the pdi-based catalyst family. In contrast, modification of the ligand core by either substitution of the pyridine nucleus by different heterocycles[8] or introduction of substituents in the ring[9–11] poses a more stringent synthetic challenge. For instance, Alt has reported an elegant but laborious multistep route to introduce ω-alkenyloxy groups in the 4-position of the pyridine ring,[9] but electron-withdrawing substituents at the heterocyclic core are usually detrimental towards the properties of the catalyst.[9,10] In spite of these problems, the pyridine 3/5- and 4-sites provide good attachment points when modification of the ligand is not intended to alter the activity of the catalyst (e.g. ligand immobilization on surfaces), since these points remain necessarily far from the metal center, in contrast to the *N*-aryl and imine positions. For these purposes, alkyl groups are the most obvious choice, given their chemical stability and electronically nearly neutral character, but they are particularly difficult to introduce. Perhaps for this reason routes towards pdi ligands displaying alkyl groups attached to the heterocycle remain essentially unexplored.[11] Recently, we disclosed a new procedure that allows the selective alkylation of 2,6-bis{[1-(2,6-diisopropylphenyl)imino]ethyl}pyridine ($^{i\mathrm{Pr}}$pdi) ligands at the pyridine 4-position by a simple one-pot procedure.[12] In this contribution, we expand our previous results, describing the synthesis of the corresponding Fe and Co complexes and their performance as ethylene polymerization catalysts.

Results and Discussion

We reported that the reaction of MnR_2 reagents with $^{i\mathrm{Pr}}$pdi at low temperatures leads to the thermally unstable dialkylmanganese species **1**, which undergoes a spontaneous rearrangement involving the migration of one of the alkyl groups from the metal center to the 4-position of the heterocyclic ring (Scheme 1).[12] These changes are marked by a characteristic color change form the dark, nearly black hue of dialkyl species **1** to the red burgundy color of the alkyl(amido)manganese(I) complex **2** (Scheme 1). The latter

[a] Instituto de Investigaciones Químicas, Universidad de Sevilla – CSIC,
c/ Americo Vespucio, 49. 41092, Seville, Spain
Fax: +34-954460565
E-mail: campora@iiq.csic.es
[b] ISMAC-C.N.R.,
Via E. Bassini 15, 20133 Milano, Italy

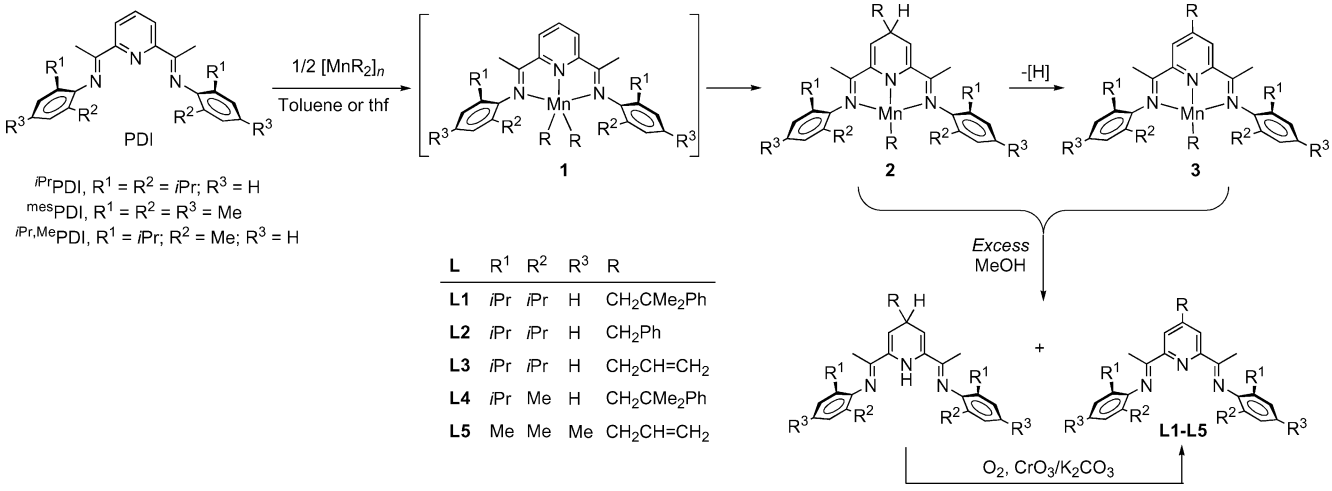

L	R^1	R^2	R^3	R
L1	*i*Pr	*i*Pr	H	CH_2CMe_2Ph
L2	*i*Pr	*i*Pr	H	CH_2Ph
L3	*i*Pr	*i*Pr	H	$CH_2CH{=}CH_2$
L4	*i*Pr	Me	H	CH_2CMe_2Ph
L5	Me	Me	Me	$CH_2CH{=}CH_2$

Scheme 1.

is prone to loss of hydrogen in solution to afford the 4-alkylated pdi derivative **3**, but this process is quite slow. Quenching the solution with methanol readily releases the modified organic ligands contained in **2** and **3** to afford a mixture of 4-alkyl-2,6-diimino-1,4-dihydropyridine and the 4-alkyl-pdi ligand. The dihydropyridine derivative is slowly aromatized on exposition to air, a reaction that is accelerated in the presence a catalytic amount of CrO_3 on K_2CO_3, which leads to the desired alkylated pdi ligand as the only significant organic product. Homoleptic or solvated dialkylmangenese(II) compounds are extremely air-sensitive species, but they can be generated and used in situ, thus avoiding their manipulation and isolation. In this way, 4-alkylated $^{i\mathrm{Pr}}$pdi derivatives **L1**–**L3** are conveniently obtained in good isolated yields.

The 1,5-alkyl migration step that takes place in the intermediate organomanganese complex is a rather unusual process, and therefore its generalization to other pdi derivatives displaying different substitution patterns at the nitrogen-bound aryl groups is not obvious. In order to expand the scope of the method, we investigated its application to two new pdi derivatives displaying decreasing degrees of steric hindrance. One of these compounds, $^{i\mathrm{Pr,Me}}$pdi, retains one *ortho*-isopropyl substituent at each of the *N*-aryl groups, while the other is replaced by a methyl group, and in the second, $^{\mathrm{Mes}}$pdi, both *ortho* and *para* positions of the *N*-aryl group are substituted by methyl groups. In both cases the reaction follows the same pathway, and ligands **L4** and **L5** were isolated in good yields without any special modification of the general procedure (see Experimental Section).

As expected, treatment of ligands **L1**, **L2**, or **L3** with suspensions of metal halides ($FeCl_2{\cdot}4H_2O$ or $CoCl_2$) in organic solvents gives rise to the corresponding complexes **4**–**9** (Scheme 2). We did not pursue the synthesis of the metal derivatives corresponding to **L4** or **L5**, although very likely they would also readily be obtained following this standard procedure. The new complexes precipitate out from the reaction media (usually thf) and are readily separated by filtration, followed by washing with hexane. Their solubility is somewhat higher than that of the parent complexes, and in some cases, the synthesis is advantageously performed in diethyl ether, rather than thf in order to ensure precipitation. The complexes are obtained as microcrystalline, paramagnetic solids with magnetic moments typical of high-spin electronic configurations (Fe complexes, $\mu_{\mathrm{eff}} \approx$ 5.3 BM; Co, $\mu_{\mathrm{eff}} \approx 4.8$ BM), and their colors are similar to those of the parent compounds, dark blue for Fe and brown for Co. Their UV/Vis spectra (CH_2Cl_2) are similar to those of the parent compounds[13] and display a single, broad absorption band in the visible region that is assigned to MLCT; the band is more intense for the iron complexes (at ca. 690 nm, $\varepsilon \approx 10^3$) than for the cobalt complexes (700 nm, $\varepsilon \approx 10^2$). A group of bands probably associated with internal pdi ligand $\pi \rightarrow \pi^*$ transitions are found in the ultraviolet range between 250 and 300 nm. The presence of the alkyl group has only a very slight effect on the position of the

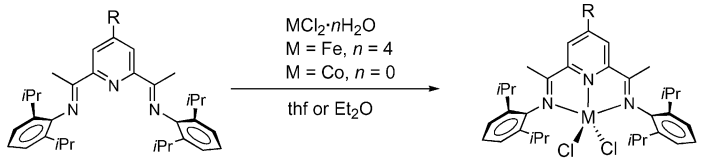

R		R	M	R	M
L1	CH_2CMe_2Ph	**4**	CH_2CMe_2Ph Fe	**7**	CH_2CMe_2Ph Co
L2	CH_2Ph	**5**	CH_2Ph Fe	**8**	CH_2Ph Co
L3	$CH_2CH{=}CH_2$	**6**	$CH_2CH{=}CH_2$ Fe	**9**	$CH_2CH{=}CH_2$ Co

Scheme 2.

UV/Vis absorption bands. The frequency of the MLCT band is expected to be more sensitive to the electronic influence of the 4-R group; however, a very small bathochromic shift of this band relative to that in $FeCl_2(^{i\mathrm{Pr}}\mathrm{pdi})$ was observed only in the Fe complexes (3 nm for **4** and 5 nm for **5** and **6**), while its position remains essentially unchanged for the Co compounds. This suggests that the presence of the alkyl substituent does not significantly perturb the electronic structure of the complexes.

The ^{1}H NMR spectra of complexes **4**–**9** display typical paramagnetically shifted signals, which are generally broader in the Fe than in the Co derivatives. All signals were assigned on the basis of their relative intensity and width and by comparison with the spectra of the corresponding $MCl_2(^{i\mathrm{Pr}}\mathrm{pdi})$ complexes. One of the most noticeable features of these spectra is the lack of the pyridine 4-H signal, which occurs at 82.4 and 116.5 ppm in the Fe and Co parent complexes, respectively. Other signals for the pdi framework are little affected by the presence of the 4-alkyl substituent. The atoms of the latter groups are farthest from the metal center, and thus they are expected to be less affected by the paramagnetism. This is true in general, and these signals usually appear sharper and occur close to the diamagnetic zone. For instance, the signal for the *para*-H atom of the benzyl group in **8** is sharp enough to allow resolution of the vicinal H–H coupling; this signal appears as a triplet at δ = 12.6 ppm with $^3J_{HH}$ = 6.5 Hz. However, the aromatic pyridine ring effectively delocalizes the spin density, and some of the resonances of the pending group may display large contact shifts, which can vary significantly from one compound to another. For instance, the ring-bound CH_2 group gives rise to a signal at δ = –13.7 ppm in **6**, –35.0 ppm in **7** and –31.1 ppm in **8**, while this signal appears within the +10 to +15 ppm region for the three cobalt derivatives.

Crystals of compounds **4** and **7** bearing a neophyl substituent in the pyridine ring were grown from CH_2Cl_2/hexane (9:1) solutions at –20 °C over several days. Their molecular structures are shown in Figure 1 and Figure 2, and selected bond lengths and angles are collected in Table 1, where they are compared with the analogous parameters in the parent complexes reported by Gibson.[1b,4c] During one attempt of crystallizing **4**, a crop of brown crystals was obtained. Its X-ray structure (Figure 3) showed it to be a mixed valence binuclear iron compound, probably arising from oxidation by adventitious traces of oxygen. An almost identical result was obtained by Brookhart and Small, who reported the analogous structure of an oxidation product isolated on attempted crystallization of a $FeCl_2$(pdi) complex.[4b]

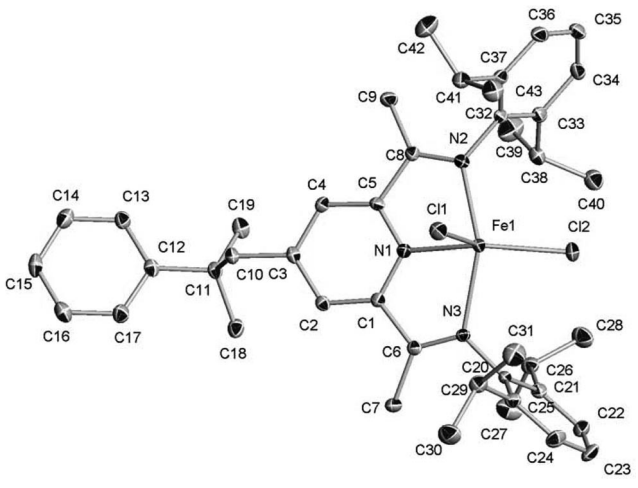

Figure 1. X-ray crystal structure of complex **4**.

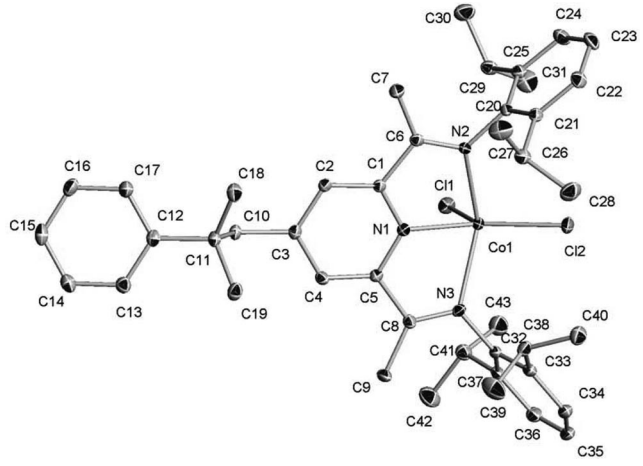

Figure 2. X-ray crystal structure of complex **7**.

Table 1. Selected bond lengths [Å] and angles [°] for complexes **4** and **7** and comparison with the parent compounds $MCl_2(^{i\mathrm{Pr}}\mathrm{pdi})$.

Bond/Angle	**4**	Δ_{Fe}[a]	**7**	Δ_{Co}[a]
M1–N1	2.0781(17)	–0.0099	2.0529(11)	0.0019
M1–N2	2.2149(16)	–0.0231	2.2090(11)	–0.002
M1–N3	2.2371(15)	–0.0129	2.2186(11)	0.0076
M1–Cl2	2.2651(6)	–0.0009	2.2554(5)	0.0044
M1–Cl1	2.3139(6)	0.0029	2.2847(4)	–0.0083
N1–C5	1.343(2)	0.005	1.3343(18)	–0.0047
N1–C1	1.342(2)	0.005	1.3377(17)	0.0007
N2–C8	1.289(3)	0.004	1.2828(17)	0.0058
N3–C6	1.284(2)	0.004	1.2866(17)	0.0066
C5–C8	1.488(2)	0.005	1.4931(18)	0.0031
C4–C5	1.385(3)	0.001	1.3921(18)	0.0091
C3–C4	1.400(3)	0.012	1.4018(18)	0.0128
C2–C3	1.398(3)	0.027	1.3955(19)	0.0265
C1–C2	1.388(3)	–0.009	1.3893(18)	–0.0077
C1–C6	1.489(3)	0.008	1.4897(19)	–0.0053
Cl1–M1–Cl2	117.64(2)	0.19	116.726(16)	0.2
N1–M1–Cl2	147.86(5)	0.00	148.60(3)	2.0
N1–M1–Cl1	95.53(4)	–0.07	94.65(3)	1.75

[a] Bond length or angle differences with the analogous parameters in corresponding $MCl_2(^{i\mathrm{Pr}}\mathrm{pdi})$ complexes (M = Fe;[1b] Co[3c]).

Compounds **4** and **7** are isomorphous and crystallize in the same point group (monoclinic C_c), with very close crystal unit parameters and identical molecular arrangements. The neophyl fragment is extended, with the essentially coplanar phenyl and pyridine rings disposed in antiperiplanar position with respect to the C11–C10 bond. The metal centers are in approximately square-pyramidal environments. The MCl_2(pdi) frameworks show only slight differences

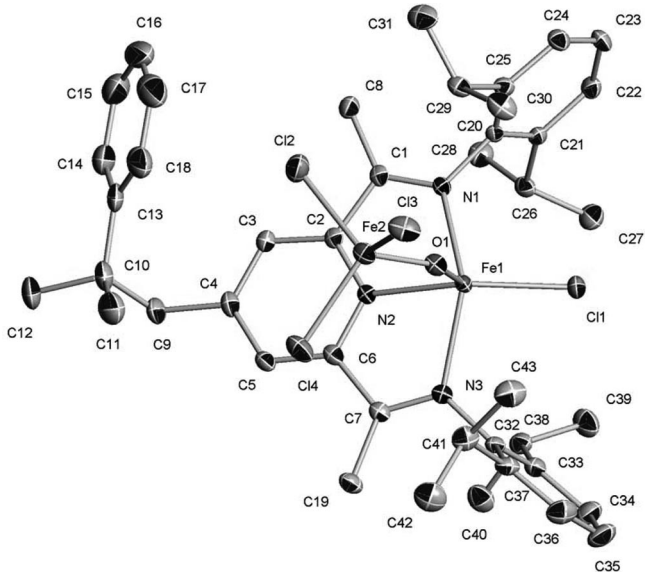

Figure 3. X ray crystal structure of complex **10**. Selected bond lengths [Å] and angles [°]: Fe1–N1 2.1725(18), Fe1–N2 2.0754(18), Fe1–N3 2.1765(18), Fe1–O1 1.7624(15), Fe1–Cl1 2.2067(6), Fe2–Cl(average) 2.2241(7), Fe1–O1–Fe2 146.7(1).

from those of the unsubstituted complexes. Thus, the average differences in the bond lengths in the substituted and unsubstituted complexes (calculated as a standard deviation over the selected bond lengths contained in Table 1) are 0.012 Å for the Fe complexes and 0.009 Å for the Co complexes, which indicate a somewhat larger variation in the former case. The C2–C3 and C3–C4 bonds, next to the alkyl group attachment point, are elongated to the same extent in **4** and **7** (0.012 and 0.027 Å) with respect to the reference complexes, possibly because of steric effects. The other bonds are almost insensitive to the presence of the alkyl group in the cobalt derivative, but some small differences can be noticed for the iron complex, notably in the Fe–N bonds which are 0.01–0.02 Å shorter in **4** than in $FeCl_2(^{i\mathrm{Pr}}\mathrm{pdi})$. The shortening of the three Fe–N bonds suggests that the alkyl substituent increases the donor capability of the pdi ligand towards the Fe^{II} center, but this is not supported by the Fe–Cl2 bond length, which would be expected to be longer because of the stronger *trans* influence of the ligand but remains the same length (within the experimental uncertainty) as in the parent compound.

Like the analogous dinuclear compound reported by Brookhart and Small, the molecule of compound **10** displays two iron centers bridged by an oxygen atom. The angular Fe–O–Fe unit [Fe1–O1–Fe2 146.7(1)°] suggests that the bridging atom does not belong to an oxido group but rather to a hydroxido group, and consequently, the compound is probably a mixed valence Fe^{II}–Fe^{III} complex. However, there is no further support for this proposal, as the IR spectrum does not show any band that might be unambiguously assigned to the hydroxido group. The conformation of the molecule of **10** in its crystal structure differs from that observed for **4** and **7**. The phenyl and pyridine groups are placed in a *gauche* position with respect to the C9–C10 bond, and the two rings have approximately perpendicular orientations. This difference could be due to crystal packing forces, imposed by the different molecular shape.

The performance of iron and cobalt complexes **4**–**9** as precatalysts for ethylene polymerization has been investigated, by using methylaluminoxane (MAO) as cocatalyst, with an M/Al ratio 1:500. The polymerization reactions were carried out under near atmospheric pressure of ethylene (1.1 bar) in magnetically stirred reactors with an exter-

Table 2. Data for ethylene polymerization experiments.[a]

Entry	Catalyst	PE yield [g]	Activity ($\times10^{-3}$)[b]	M_n ($\times10^{-3}$)[c]	M_w ($\times10^{-3}$)[c]	M_w/M_n[c]	M_v ($\times10^{-3}$)
1	$FeCl_2(^{i\mathrm{Pr}}\mathrm{pdi})$	1.0	1.4	9.2	62.6	6.8	63.0[c]
2	$FeCl_2(^{i\mathrm{Pr}}\mathrm{pdi})$	1.1	1.5				46.1[d]
3	$FeCl_2(^{i\mathrm{Pr}}\mathrm{pdi})$	1.3	1.8				
4	$FeCl_2(^{i\mathrm{Pr}}\mathrm{pdi})$	1.2	1.6				
5	**4**	1.1	1.5	10.6	83.7	7.9	84.1[c]
6	**4**	1.4	1.9	7.3	37.2	5.1	37.1[c]
7	**5**	0.8	1.1	13.4	56.1	4.2	56.0[c]
8	**5**	1.1	1.5				34.6[d]
9	**6**	1.4	1.9	7.1	176.1	24.8	175.3[c]
10	**6**	1.2	1.6	8.4	179.7	21.4	180.0[c]
11	**6**	1.1	1.5				182.0[d]
12	$CoCl_2(^{i\mathrm{Pr}}\mathrm{pdi})$	0.9	1.2	10.9	29.4	2.7	29.5[c]
13	$CoCl_2(^{i\mathrm{Pr}}\mathrm{pdi})$	0.8	1.1	11.9	33.3	2.8	28.4[c]
14	**7**	0.7	1.0				
15	**7**	0.6	0.8				
16	**8**	0.7	1.0				20.7[d]
17	**8**	0.6	0.8	10.4	25.7	2.7	28.1[c]
18[e]	**9**	0.7	1.0				
19[e]	**9**	0.5	0.7				
20[e]	**9**	0.8	1.1				

[a] Polymerization conditions: catalyst amount, 4 μmol; solvent, toluene (100 mL); external bath temperature, 30 °C; ethylene pressure, 1.1 bar; cocatalyst, MAO (M/Al = 1:500); reaction time, 10 min. [b] Activity in kg PE (mol catalyst)$^{-1}$ bar^{-1} h^{-1}. [c] Determined by GPC. [d] Determined by viscosimetry. [e] Insoluble polymer.

nal bath thermostated at 30 °C. Catalytic activities and polymer characterization data are collected in Table 2. For comparison, Table 2 includes polymerization data corresponding to the reference complexes $FeCl_2(^{i\text{Pr}}pdi)$ and $CoCl_2(^{i\text{Pr}}pdi)$ under the same experimental conditions as those employed for their functionalized derivatives. In our hands, the behavior of these two catalysts matches that reported in the literature, although the activity figures are somewhat lower.[1,3] In general, the iron catalysts produce higher molecular weight polymers than their cobalt analogues, but with a markedly broader molecular weight distribution. As expected, the iron catalysts are significantly more active than the cobalt catalysts. Previously reported $FeCl_2(^{i\text{Pr}}pdi)$ catalysts bearing electron-withdrawing groups in the pyridine 4-position (OR,[9] Cl[10]) show activities that are significantly lower than those of their unsubstituted congeners. In contrast, the 4-alkylated Fe derivatives **4**–**6** maintain essentially unaltered activities, and a similar conclusion can be drawn for the cobalt analogues **7**–**9**. The polymer samples generated by the Fe and Co neophyl and benzyl derivatives show insignificant variations in the molecular weight and polydispersity that can be attributed to changes in the internal reactor temperature during the experiments. However, both the Fe and Co allyl derivatives **6** and **9** produce appreciably less-soluble polyethylene samples, a feature that suggests they have higher molecular weights. Although this fact prevented the characterization of the polymers obtained with **9**, GPC and viscosimetric analysis of the product of the iron catalyst **6** (Entries 9 and 10) confirms a substantial increase in M_w and M_v, to ca. 180000. The GPC traces of these polymers indicate very broad, bimodal molecular weight distributions, with peaks at M_p = 68000 (major) and 890. At this point, it is difficult to give a reasonable explanation for these findings, but the presence of a polymerizable vinyl unit in the structure of **6** and **9** suggests that these catalysts might become incorporated in the growing polymer chain, which leads to a somewhat modified propagating species. Alt demonstrated this possibility for metallocene catalysts containing pending alkenyl chains attached to the Cp ligands. This so-called self-immobilization of the catalyst usually results in substantially modified activities and polymer structures.[14] The concept of self-immobilization has been extended to other catalytic systems that include late transition metals.[3] Herrmann[15] and Jin[16] functionalized $FeCl_2$(pdi) complexes with alkenyl chains at the α-imino or the *N*-aryl positions, respectively, and they obtained some evidence of the self-immobilization phenomena in spite of the poor capability of iron catalysts for α-olefin incorporation.[4b,4d,17] For instance, Jin mentioned the production of polymers with large polydispersity indexes (M_w/M_n) of up to 22, which are similar to those generated by **6**. In contrast, Alt reported that catalysts modified with pending *O*-alkenyl groups at the 4-position of the pyridine ring produce polyethylenes with a monomodal molecular weight distribution, in contrast with the bimodal polymers obtained with the analogous nonfunctionalized catalysts. The presence of the 4-alkenoxy group was also found to be beneficial in that it helps to prevent fouling of the reactor.[9] Alt recently described the synthesis and catalytic activity of a wide range of $FeCl_2$(pdi) complexes similar to those previously reported by the Herrmann and Jin groups, but, somewhat paradoxically, no conclusive evidence of catalyst self-immobilization was found.[18] In order to obtain some additional evidence of the existence of unusual effects on the catalytic behavior of the 4-allyl-functionalized complexes **6** and **9**, we decided to examine the morphology of the polymers generated with these catalysts by using scanning electron microscopy (SEM). Self-immobilization of catalysts is thought to lead the formation of microscopic polymer particles, which mimic the initial immobilized catalyst seeds. As an example of this behavior, Jin mentioned the production of micron-sized spheres when using either nickel or iron catalysts bearing pending alkenyl groups.[16] Figure 4 shows SEM images of polymer samples prepared with the two 4-allyl-functionalized pyridine catalysts and those generated with the $FeCl_2(^{i\text{Pr}}pdi)$ and $CoCl_2(^{i\text{Pr}}pdi)$ reference complexes. The latter complexes give rise to rather structured polymer materials in the 1–2 micron scale (Figure 4C and D, respectively). The cobalt catalyst gives formations that resemble platelet clusters, whilst the iron catalyst gives rise to partially spherical, hollow, "shell-like" particles, which are likely to consist of curved lamellae. It seems likely that these structures arise from the partially crystalline character of the materials, particularly in the case of those produced with the cobalt catalyst, since this catalyst gives relatively small polyethylene molecules with a narrow molecular weight distribution. In contrast, the images of the polymers produced with **6** and **9** appear to be more homogeneous and lack structural features (Figure 4A and B). This might possibly be attributed to the higher molecular weight and wider range of molecular sizes (at least in the case of the Fe catalyst), which results in an amorphous material. However, it seems clear that the images provide no evidence of polymer particles resulting from catalyst self-immobilization.

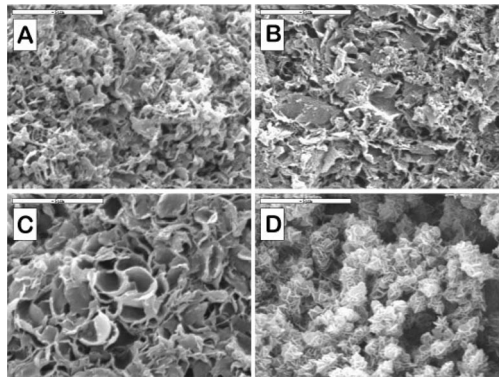

Figure 4. SEM images of polyethylene samples produced with complexes **6** (A) and **9** (B) and with the reference complexes $FeCl_2(^{i\text{Pr}}pdi)$ (C) and $CoCl_2(^{i\text{Pr}}pdi)$ (D). The bar scale represents 5 μm.

Summary and Conclusions

Several pdi ligands displaying alkyl substituents at the 4-position of the central pyridine ring have been prepared by a simple procedure involving the reaction of in situ generated MnR_2 reagents with readily available nonfunctionalized ligands. The scope of the method has been expanded, thus allowing the synthesis of new 4-alkylated pdi ligands displaying *N*-aryl substituents with different degrees of steric hindrance. A set of Fe and Co complexes (**4**–**9**) containing 4-R pdi ligands (R = neophyl, benzyl, and allyl) have been synthesized and fully characterized. The presence of the alkyl substituent at the pyridine ring increases the solubility of the new complexes relative to the corresponding parent complexes, but it has very minor effect on their structures and physical properties. The impact of the alkyl substituent on the catalytic properties of the 4-neophyl and 4-benzyl derivatives in ethylene polymerization is also negligible. This suggests that our methodology would be advantageous for the introduction of special groups suitable for immobilization, in comparison with other methods in which the linker functionality is placed in positions where it may have a significant influence on the catalyst activity. Similarly to the neophyl and benzyl groups, introduction of a 4-allyl group on the pyridine ring does not alter the productivity of the corresponding Fe and Co catalysts (**6** and **9**), but the polymers generated by them are appreciably less soluble. GPC analyses of the polymer produced by catalyst **6** shows much larger values of M_w (up to 180000) and a larger polydispersity index (M_w/M_n = 21). The origin of this effect is currently unknown, but it is conceivable that a self-immobilization phenomenon, arising from the copolymerization of the pending allyl group into the growing polyethylene chain, could be involved.

Experimental Section

All preparations were carried out under oxygen-free nitrogen by conventional Schlenk techniques or in a nitrogen-filled glove-box unless otherwise stated. Microanalyses were performed by the Microanalytical Service of the Instituto de Investigaciones Químicas (Sevilla, Spain). Infrared spectra were recorded on a Bruker Vector 22, UV/Vis spectra on a Perkin–Elmer Lambda 12 spectrophotometer, and NMR spectra on Bruker DRX 300, 400 and 500 MHz spectrometers. The ^1H and $^{13}C\{^1H\}$ resonances of the solvent were used as the internal standard, but the chemical shifts are reported with respect to TMS. Magnetic susceptibility measurements were made on a Sherwood Scientific balance model MSB-Auto. HPLC grade organic solvents were freshly distilled prior to use. Diethyl ether and thf were distilled from sodium benzophenone. CH_2Cl_2 was distilled from CaH_2, and hexane, toluene, and benzene from sodium benzophenone ketyl. Upon collection, all of them were deoxygenated prior to use.

The molar mass distribution (MMD) and polydispersity measurements were performed on a high temperature dual-detector size exclusion chromatography (SEC) system. The SEC system was a GPCV2000 from Waters (Milford, MA) that uses two on-line detectors: a differential viscometer (DV) and a differential refractometer (DRI) as concentration detector. The experimental conditions were as follows: *o*-dichlorobenzene + 0.05% 2,6-di-*tert*-butyl-4-methylphenol (BHT, antioxidant) as mobile phase, 0.8 mL/min as flow rate, and a column temperature of 145 °C. The column set was composed of three GMHXL-HT columns from Toso Haas (Stuttgart, Germany). The universal calibration was constructed from 18 narrow MMD polystyrene standards, with the molar mass ranging from 162 to 5.48×10^6 g/mol. The MM values reported are those obtained with the DV detector. Methylaluminoxane (MAO) was purchased from Aldrich as a 7-% solution in heptane. The pdi ligands were synthesized from 2,6-diacetylpyridine according to standard procedures. The preparation of derivatives $^{i\mathrm{Pr}}$pdi-4-R [where R = CH_2CMe_2Ph (**L1**); CH_2Ph (**L2**); $CH_2CH{=}CH_2$ (**L3**)] was carried out following the synthetic method reported by us in the literature.[10] $FeCl_2{\cdot}4H_2O$ and $CoCl_2$ were purchased from Aldrich and used without further purification. The synthesis of $FeCl_2(^{i\mathrm{Pr}}\mathrm{pdi})$ and $CoCl_2(^{i\mathrm{Pr}}\mathrm{pdi})$ was carried out as shown below for other complexes. UV/Vis data (CH_2Cl_2): $FeCl_2(^{i\mathrm{Pr}}\mathrm{pdi})$, λ_{max} (ε, $M^{-1}\,cm^{-1}$) = 294 (3800), 365 sh. (740), 689 (1300) nm; $CoCl_2(^{i\mathrm{Pr}}\mathrm{pdi})$, λ_{max} (ε, $M^{-1}\,cm^{-1}$) = 293 (3800), 362 (1100), 445 sh. (460), 701 (110) nm.

Synthesis of 4-Allyl-2,6-bis[1-(mesitylimino)ethyl]pyridine (L5): A pink suspension of thf (20 mL) and anhydrous $MnCl_2$ (326 mg, 2.61 mmol) was treated with $Mg(CH_2CH{=}CH_2)Cl$ (4.21 mL of a 1.3 M solution) in diethyl ether (5.5 mmol, 2.1 equiv.) at –78 °C. The mixture was stirred for 10 min and it turned pale green. The cooling bath was removed, and as the mixture warmed up, its color changed from pale green to brown. The color changed again to pale yellow while stirring at room temperature for 10–15 min. The solution, containing the "$Mn(CH_2CH{=}CH_2)_2$" reagent, was transferred to a yellow solution of $^{\mathrm{Mes}}$pdi (884 mg, 2.08 mmol) in thf (60 mL) stirred at –78 °C. This resulted in an instantaneous color change to dark brown. Vigorous stirring was continued for 10 min at –78 °C, and then the mixture was warmed to room temperature. On continued stirring for 90 min, its color changed to deep purple, and then it was quenched with excess anhydrous methanol (8–10 mL) and the solvents evaporated under vacuum. The remaining orange oil was extracted with hexane (3×25 mL) and toluene (2×20 mL), and the extracts were filtered from a brown precipitate. The oily mixture was taken up in thf (100 mL) and stirred in air with a catalytic amount of CrO_3/K_2CO_3 (10%) for 1 h at room temperature. After evaporation, the oil was dissolved in hexane and evaporated again to dryness to afford **L4** as a yellow solid. Yield: 0.71 g (78%). ^1H NMR ($CDCl_3$, 298 K, 300 MHz): δ = 8.29 (s, 2 H, *m*-CH_{py}), 6.79 (s, 4 H, $CH_{ar(aniline)}$) 3.00 (s, 2 H, CH_2CMe_2Ph), 5.93–5.84 (m, 1 H, $CH_2CH{=}CH_2$), 5.13–5.08 (m, 2 H, $CH_2CH{=}CH_2$), 3.47 (m, 2 H, $CH_2CH{=}CH_2$), 2.37 (s, 6 H, $CH_3C{=}N$), 1.91 (s, 6 H, *o*-CH_3) 1.83 (s, 6 H, *m*-CH_3), 1.81 (s, 6 H, *p*-CH_3) ppm. ESI-MS: m/z = 438.3 $[M + 1]^+$.

Synthesis of 2,6-Bis{[1-(2-isopropyl-6-methylphenyl)imino]ethyl}-4-neophylpyridine (L4): A pink suspension of thf (20 mL) and anhydrous $MnCl_2$ (187 mg, 1.48 mmol) was treated with $Mg(CH_2CMe_2Ph)Cl$ (2.43 mL of a 1.3 M solution) in diethyl ether (3.16 mmol, 2.1 equiv.) at –78 °C. The mixture was stirred for 10 min and it turned pale green. The cooling bath was removed, and as the mixture warmed up, its color changed from pale green to brown. The color changed again to pale yellow while stirring at room temperature for 10–15 min. The solution, containing the "$Mn(CH_2CMe_2Ph)_2$" reagent, was transferred to a yellow suspension of $^{i\mathrm{Pr,Me}}$pdi (580 mg, 1.19 mmol) in thf (60 mL) stirred at –78 °C. This resulted in an instantaneous color change to dark brown. Vigorous stirring was continued for 10 min at –78 °C, and then the mixture was warmed to room temperature. On continued stirring for 90 min, its color changed to deep purple, and then it

was quenched with excess anhydrous methanol (8–10 mL) and the solvents evaporated under vacuum. The remaining orange oil was extracted with hexane (3 × 25 mL) and toluene (2 × 20 mL), and the extracts were filtered from a brown precipitate. The filtrate was dried, and the resulting oil (0.65 g, 89%) was found by NMR spectroscopy to consist of a mixture of **L5** and the corresponding dihydropyridine in a relative ratio of 1:2. The oily mixture was taken up in thf (100 mL) and stirred in air with a catalytic amount of CrO_3/K_2CO_3 (10%) for 1 h at room temperature. After evaporation, the residue was crystallized from hexane. Yield: 0.52 g (71%). ^{1}H NMR ($CDCl_3$, 298 K, 300 MHz): δ = 7.95 (s, 2 H, *m*-CH_{py}), 7.28–6.99 (m, 11 H, C$H_{ar(Ph)}$ and C$H_{ar(neof)}$), 3.00 (s, 2 H, CH_2CMe$_2$Ph), 2.72 [sept, $^3J_{HH}$ = 5.4 Hz, 2 H, CH(CH$_3$)$_2$], 2.24 (s, 6 H, CH_3C=N), 1.95 (s, 6 H, *o*-CH_3), 1.17 (s, 6 H, CH$_2$CMe_2Ph), 1.14 (d, $^3J_{HH}$ = 5.4 Hz, 6 H), 1.10 [d, $^3J_{HH}$ = 5.4 Hz, 6 H, CH(CH_3)$_2$] ppm. ^{13}C{^{1}H} NMR: δ = 17.1 (*C*H$_3$C=N), 18.4 (Me$_{ar}$) 23.1, 23.4 (CHMe_2), 28.5 (CH$_2$CMe_2Ph), 29.3 (*C*HMe$_2$), 39.1 (CH$_2$*C*Me$_2$Ph), 50.8 (*C*H$_2$CMe$_2$Ph), 123.4 (3,5-*C*$_{ar}$), 124.2 (4-*C*$_{ar}$), 125.3 (3,5-*C*$_{ar(py)}$), 126.1 (4-*C*$_{ar(Ph)}$), 127.9 (2,6-*C*$_{ar(Ph)}$), 128.3 (3,5-*C*$_{ar(Ph)}$), 136.6 (*C*$_{ar}$), 147.8 (*C*$_{ar}$), 147.9 (*C*$_{ar(py)}$), 148.9 (*C*$_{ar}$), 154.6 (*C*$_{ar(py)}$), 167.4 (CH$_3$*C*=N) ppm. IR (Nujol mull): ν(C=N) = 1643, 1619, 1591, 1555 cm^{-1}.

Synthesis of FeCl$_2$(L1) (4): A thf solution (10 mL) of **L1** (0.674 g, 1.1 mmol) was added dropwise to a stirred suspension of $FeCl_2 \cdot 4H_2O$ (0.198 g, 1 mmol) in thf (10 mL) at room temperature. The mixture turned from yellow to green. The suspension was stirred for 24 h at room temperature, and the green solid was removed by filtration and washed with hexane (2 × 10 mL) and dried in vacuo to obtain 0.8 g of a green powdery solid. Yield: 693 mg (85%). ^{1}H NMR (CD_2Cl_2, 298 K, 300 MHz): δ = 84.60 ($\Delta\nu_{1/2}$ = 156 Hz, 2 H, 3,5-CH_{py}), 14.59 ($\Delta\nu_{1/2}$ = 37 Hz, 4 H, *m*-CH_{ar}), 11.08 ($\Delta\nu_{1/2}$ = 37 Hz, 2 H, *m*-C$H_{ar(neof)}$), 8.65 ($\Delta\nu_{1/2}$ = 32 Hz, 2 H, *o*-C$H_{ar(neof)}$), 7.25 ($\Delta\nu_{1/2}$ = 32 Hz, 1 H, *p*-C$H_{ar(neof)}$), 5.04 ($\Delta\nu_{1/2}$ = 37 Hz, 6 H, CMe_2), –4.83 [$\Delta\nu_{1/2}$ = 87 Hz, 12 H, CH(CH_3)$_2$], –6.13 [$\Delta\nu_{1/2}$ = 41 Hz, 12 H, CH(CH_3)$_2$], –10.33 ($\Delta\nu_{1/2}$ = 41 Hz, 2 H, *p*-CH_{ar}) –13.74 ($\Delta\nu_{1/2}$ = 105 Hz, 2H, C$H_{2(neof)}$) –23.07 [$\Delta\nu_{1/2}$ = 344 Hz, 4 H, CH(CH$_3$)$_2$], –27.39 ($\Delta\nu_{1/2}$ = 170 Hz, 6 H, CH_3C=N) ppm. IR (Nujol mull): ν(C=N) = 1625, 1590 cm^{-1}. UV/Vis (CH_2Cl_2): λ_{max} (ε, M^{-1} cm^{-1}) = 298 (3800), 309 sh. (8100), 360 sh. (4600), 689 (1400) nm. μ_{eff} (magnetic susceptibility balance, 293 K) = 5.39 μ_B.

Attempts to grow crystals of this compound from a CH_2Cl_2/hexane (9:1) mixture also afforded a crop of brown crystals of compound **10**.

Synthesis of FeCl$_2$(L2) (5): The synthesis of this compound was carried out in the same manner and scale as that of **4**, but with **L2**. Yield: 0.35 g (45%). ^{1}H NMR (CD_2Cl_2, 298 K, 300 MHz): δ = 83.40 ($\Delta\nu_{1/2}$ = 41 Hz, 2 H, 3,5-CH_{py}), 14.45 ($\Delta\nu_{1/2}$ = 18 Hz, 4 H, *m*-CH_{ar}), 13.22 ($\Delta\nu_{1/2}$ = 18 Hz, 2 H, *m*-CH_{Bz}), 9.68 ($\Delta\nu_{1/2}$ = 18 Hz, 2 H, *o*-CH_{Bz}), 9.31($\Delta\nu_{1/2}$ = 18 Hz, 1 H, *o*-CH_{Bz}), –5.58 [$\Delta\nu_{1/2}$ = 55 Hz, 12 H, CH(CH_3)$_2$], –6.76 [$\Delta\nu_{1/2}$ = 18 Hz, 12 H, CH(CH_3)$_2$], –10.59 ($\Delta\nu_{1/2}$ = 23 Hz, 2 H, *p*-CH_{ar}), –25.16 [$\Delta\nu_{1/2}$ = 234 Hz, 4 H, CH(CH$_3$)$_2$], –32.74 ($\Delta\nu_{1/2}$ = 36 Hz, 6 H, CH_3C=N), –35.04 ($\Delta\nu_{1/2}$ = 14 Hz, 2 H, C$H_{2(Bz)}$) ppm. IR (Nujol mull): ν(C=N) = 1593 cm^{-1}. UV/Vis (CH_2Cl_2): λ_{max} (ε, M^{-1} cm^{-1}) = 296 (6700), 305 sh. (6200), 367 sh. (2300), 689 (2200) nm. μ_{eff} (magnetic susceptibility balance, 293 K) = 5.24 μ_B. $C_{40}H_{49}Cl_2FeN_3$ (697.25): calcd. C 68.77, H 7.07, N 6.02; found C 68.55, H 7.35, N 6.08.

Synthesis of FeCl$_2$(L3) (6): The synthesis of this compound was carried out in a similar manner to that of **4**, but with diethyl ether as solvent and **L3**. Yield: 0.41 g of a blue solid (58%). ^{1}H NMR (CD_2Cl_2, 298 K, 400 MHz): δ = 83.83 ($\Delta\nu_{1/2}$ = 83 Hz, 2 H, 3,5-CH_{py}), 14.29 ($\Delta\nu_{1/2}$ = 24 Hz, 4 H, *m*-CH_{ar}), 13.79 ($\Delta\nu_{1/2}$ = 44 Hz, 1 H, CH_2=CHCH$_2$), 10.32 ($\Delta\nu_{1/2}$ = 34 Hz, 1 H, CH_2=CHCH$_2$), 7.72 ($\Delta\nu_{1/2}$ = 24 Hz, 1 H, CH$_2$=CHCH$_2$), –5.44 [$\Delta\nu_{1/2}$ = 73 Hz, 12 H, CH(CH_3)$_2$], –6.59 [$\Delta\nu_{1/2}$ = 29 Hz, 12 H, CH(CH_3)$_2$], –10.49 ($\Delta\nu_{1/2}$ = 24 Hz, 2 H, *p*-CH_{ar}), –24.56 [$\Delta\nu_{1/2}$ = 290 Hz, 4 H, CH(CH$_3$)$_2$], –30.24 ($\Delta\nu_{1/2}$ = 78 Hz, 6 H, CH_3C=N), –31.09 ($\Delta\nu_{1/2}$ = 68 Hz, 2 H, CH$_2$=CHCH_2) ppm. IR (Nujol): ν(C=N) = 1596 cm^{-1}. UV/Vis (CH_2Cl_2): λ_{max} (ε, M^{-1} cm^{-1}) = 300 (4600), 304 sh. (4500), 369 sh. (1800), 692 (2500) nm. $C_{36}H_{47}Cl_2FeN_3$ (647.25): calcd. C 66.77, H 7.30, N 6.48; found C 65.11, H 7.12, N 6.12.

Synthesis of CoCl$_2$(L1) (7): A thf solution (10 mL) of **L1** (0.674 g, 1.1 mmol) was added dropwise to a stirred suspension of $CoCl_2$ (0.128 g, 1 mmol) in thf (10 mL) at room temperature. The resulting mixture turned from blue to brown. The suspension was stirred for 24 h at room temperature, and the dark brown solid was filtered out, washed with hexane (2 × 10 mL), and dried under vacuum to yield 0.8 g of a brown powdery solid, which was recyrstallized from CH_2Cl_2/hexane (9:1) at –30 °C. Yield: 0.43 g (58%). ^{1}H NMR: δ = 114.83 ($\Delta\nu_{1/2}$ = 92 Hz, 2 H, 3,5-CH_{py}), 26.04 ($\Delta\nu_{1/2}$ = 17 Hz, 2 H, *m*-C$H_{ar(neof)}$), 20.15 ($\Delta\nu_{1/2}$ = 21 Hz, 2 H, *o*-C$H_{ar(neof)}$), 14.66 ($\Delta\nu_{1/2}$ = 15 Hz, 6 H, C$Me_{2(neof)}$), 10.84 ($\Delta\nu_{1/2}$ = 22 Hz, 2 H, CH$_{2(neof)}$), 8.70 ($\Delta\nu_{1/2}$ = 17 Hz, 1 H, *p*-C$H_{ar(neof)}$), 8.09 ($\Delta\nu_{1/2}$ = 18 Hz, 4 H, CH_{ar}), 2.10 ($\Delta\nu_{1/2}$ = 34 Hz, 6 H, CH_3C=N$_{ar}$), –9.41 ($\Delta\nu_{1/2}$ = 27 Hz, 2 H, *p*-CH_{ar}), –18.86 [$\Delta\nu_{1/2}$ = 29 Hz, 24 H, CH(CH_3)$_2$], –88.32 [s, 2 H, CH(CH$_3$)$_2$] ppm. IR (Nujol mull): ν(C=N) = 1597 cm^{-1}. UV/Vis (CH_2Cl_2): λ_{max} (ε, M^{-1} cm^{-1}) = 302 (4500), 356 (1800), 434 sh. (800), 703 (150) nm. μ_{eff} (magnetic susceptibility balance, 293 K) = 4.67 μ_B. $C_{43}H_{55}Cl_2CoN_3$ (742.31): calcd. C 69.44, H 7.45, N 5.65; found C 69.15, H 7.50, N 5.11.

Synthesis of CoCl$_2$(L2) (8): The synthesis of this complex was carried out in the same manner as that for 7, but with **L2**. Yield: 0.26 g (45%). ^{1}H NMR (CD_2Cl_2, 298 K, 300 MHz): δ = 116.28 ($\Delta\nu_{1/2}$ = 71 Hz, 2 H, *m*-CH_{py}), 24.10 ($\Delta\nu_{1/2}$ = 16 Hz, 2 H, *m*-CH_{Bz}), 24.00 ($\Delta\nu_{1/2}$ = 16 Hz, 2 H, *o*-CH_{Bz}), 14.50 ($\Delta\nu_{1/2}$ = 16 Hz, 2 H, CH_2, Bz), 12.61 (t, $^3J_{HH}$ = 6.7 Hz, 1 H, *p*-CH_{Bz}), 8.91 ($\Delta\nu_{1/2}$ = 18 Hz, 4 H, *m*-CH_{ar}), 3.37 ($\Delta\nu_{1/2}$ = 27 Hz, 6 H, CH_3C=N), –9.18 ($\Delta\nu_{1/2}$ = 27 Hz, 2 H, *p*-CH_{ar}), –18.62 [$\Delta\nu_{1/2}$ = 14 Hz, 12 H, CH(CH_3)$_2$], –19.52 [$\Delta\nu_{1/2}$ = 66 Hz, 12 H, CH(CH_3)$_2$] –88.75[$\Delta\nu_{1/2}$ = 255 Hz, 4 H, CH(CH$_3$)$_2$] ppm. IR (Nujol): ν(C=N) = 1597 cm^{-1}. UV/Vis (CH_2Cl_2): λ_{max} (ε, M^{-1} cm^{-1}) = 300 (4800), 357 (2100), 435 sh. (980), 703 (190) nm. μ_{eff} (magnetic susceptibility balance, 293 K) = 4.90 μ_B. $C_{40}H_{49}Cl_2CoN_3$ (700.26): calcd. C 68.47, H 7.04, N 5.99; found C 67.89, H 6.86, N 5.73.

Synthesis of CoCl$_2$(L3) (9): This compound was obtained in the same manner as that described for the synthesis of **7** and **8**, as a crystalline brown solid. Yield: 0.36 g (55%). ^{1}H NMR (CD_2Cl_2, 298 K, 300 MHz): δ = 116.26 ($\Delta\nu_{1/2}$ = 117 Hz, 2 H, *m*-CH_{py}), 25.35 ($\Delta\nu_{1/2}$ = 71 Hz, 1 H, CH$_2$=CHCH$_2$), 23.49 ($\Delta\nu_{1/2}$ = 47 Hz, 2 H, CH$_2$=CHCH_2), 19.74 ($\Delta\nu_{1/2}$ = 51 Hz, 1 H, CH_2=CHCH$_2$), 15.42 ($\Delta\nu_{1/2}$ = 47 Hz, 1 H, CH_2=CHCH$_2$), 8.9 ($\Delta\nu_{1/2}$ = 51 Hz, 4 H, *m*-CH_{ar}), 3.40 ($\Delta\nu_{1/2}$ = 68 Hz, 6 H, CH_3C=N), –9.17 ($\Delta\nu_{1/2}$ = 53 Hz, 2 H, *p*-CH_{ar}), –18.66 [$\Delta\nu_{1/2}$ = 47 Hz, 12 H, CH(CH_3)$_2$], –19.45 [$\Delta\nu_{1/2}$ = 108 Hz, 12 H, CH(CH_3)$_2$], –89.09 [$\Delta\nu_{1/2}$ = 438 Hz, 4 H, CH(CH$_3$)$_2$] ppm. IR (Nujol): ν(C=N) = 1598 cm^{-1}. UV/Vis (CH_2Cl_2): λ_{max} (ε, M^{-1} cm^{-1}) = 299 (6900), 350 (2300), 430 sh. (980), 703 (150) nm. μ_{eff} (magnetic susceptibility balance, 293 K) = 4.79 μ_B. $C_{36}H_{47}Cl_2CoN_3$ (650.25): calcd. C 66.36, H 7.27, N 6.45; found C 65.79, H 7.29, N 6.24.

X-ray Structure Determination

Crystal Data for 4: $C_{44}H_{57}Cl_4FeN_3$ [$C_{43}H_{55}Cl_2FeN_3$, CH_2Cl_2], M_w = 825.58. A single crystal of suitable size, green block (0.19 × 0.13 × 0.10 mm) from CH_2Cl_2/thf, coated with dry perfluo-

ropolyether, was mounted on a glass fiber and fixed in a cold nitrogen stream, 100(2) K, to the goniometer head. Monoclinic, space group *Cc* (no. 9), a = 22.5569(19) Å, b = 12.1920(9) Å, c = 17.623(3) Å, β = 119.276(2)°, V = 4227.5(9) Å^3, Z = 4, $\rho_{calcd.}$ = 1.297 g cm^{-3}, λ(Mo-$K_{\alpha1}$) = 0.71073 Å, F(000) = 1744, μ = 0.644 mm^{-1}. 29461 Reflections were collected from a Bruker-Nonius X8Apex-II CCD diffractometer in the range $5.72 < 2\theta < 61.00°$, and 12129 independent reflections [R(int) = 0.0482] were used in the structural analysis. The data were reduced (SAINT) and corrected for Lorentz polarisation effects and absorption by the multiscan method applied by SADABS.[19,20] The structure was solved by direct methods (SIR-2002)[21] and refined against all F^2 data by full-matrix least-squares techniques (SHELXL97)[22] converged to final R_1 = 0.0396 [$I > 2\sigma(I)$] and wR_2 = 0.0808 for all data, with a goodness-of-fit on F^2, S = 0.996 and 469 parameters.

Crystal Data for 7: $C_{44}H_{57}Cl_4CoN_3$ [$C_{43}H_{55}Cl_2CoN_3$, CH_2Cl_2], M_w = 828.66. A single crystal of suitable size, red prism (0.48 × 0.14 × 0.13 mm) from CH_2Cl_2, coated with dry perfluoropolyether, was mounted on a glass fiber and fixed in a cold nitrogen stream, 100(2) K, to the goniometer head. Monoclinic, space group *Cc* (no. 9), a = 22.4998(16) Å, b = 12.1667(9) Å, c = 17.618(2) Å, β = 119.213(2)°, V = 4209.5(6) Å^3, Z = 4, $\rho_{calcd.}$ = 1.308 g cm^{-3}, λ(Mo-$K_{\alpha1}$) = 0.71073 Å, F(000) = 1748, μ = 0.696 mm^{-1}. 53090 Reflections were collected from a Bruker-Nonius X8Apex-II CCD diffractometer in the range $5.74 < 2\theta < 61.14°$, and 12060 independent reflections [R(int) = 0.0329] were used in the structural analysis. Data reduction, solving and refinement was performed in the same manner as that for **4** converged to final R_1 = 0.0270 [$I > 2\sigma(I)$] and to wR_2 = 0.0647 for all data, with a goodness-of-fit on F^2, S = 1.047 and 469 parameters.

Crystal Data for 10: $C_{43}H_{55}Cl_4Fe_2N_3O$, M_w = 883.40. A single crystal of suitable size, orange needle (0.58 × 0.15 × 0.12 mm) from CH_2Cl_2/thf/hexane, coated with dry perfluoropolyether, was mounted on a glass fiber and fixed in a cold nitrogen stream, 100(2) K, to the goniometer head. Monoclinic, space group *C*2/*c* (no. 15), a = 30.4435(14) Å, b = 17.1922(8) Å, c = 23.7690(18) Å, β = 128.0240(10)°, V = 9800.0(10) Å^3, Z = 8, $\rho_{calcd.}$ = 1.197 g cm^{-3}, λ(Mo-$K_{\alpha1}$) = 0.71073 Å, F(000) = 3696, μ = 0.842 mm^{-1}. 58740 Reflections were collected from a Bruker-Nonius X8Apex-II CCD diffractometer in the range $4.28 < 2\theta < 52.80°$, and 9959 independent reflections [R(int) = 0.0531] were used in the structural analysis. Data reduction, solving and refinement was performed in the same manner as that for **4** converged to final R_1 = 0.0353 [$I > 2\sigma(I)$] and to wR_2 = 0.0974 for all data, with a goodness-of-fit on F^2, S = 1.054 and 490 parameters.

CCDC-666530 for **4**, CCDC-666531 for **7**, and CCDC-666532 for **10** contain the supplementary crystallographic data for this paper. These data can be obtained free of charge from The Cambridge Crystallographic Data Centre via www.ccdc.cam.ac.uk/data_request/cif.

Ethylene Polymerization Experiments: Polymerization reactions were carried out in round-bottom flasks connected to a vacuum line operating with ethylene. The temperature was maintained with an external water bath thermostated at 30 °C. After the flasks were evacuated for 15 min, they were charged with toluene (100 mL) and flushed with ethylene at the line pressure (1.1 bar). A solution of the cocatalyst (MAO, 500 equiv.) was added from a pipette, followed by a solution of CH_2Cl_2 (2 mL) and precatalyst (4 μmol). After stirring for 10 min, the reaction mixture was quenched with acidified ethanol. The resultant polymer was filtered and dried in a vacuum oven at 50 °C until a constant weight was obtained.

Acknowledgments

Financial support from the Ministerio de Educación y Ciencia (Project PPQ2003-000975) and Junta de Andalucía is gratefully acknowledged. Support for personnel exchange from the European Union Network of Excellence IDECAT (contract No NMP3-CT-2005-011730) is gratefully acknowledged. A. R.-D. thanks the Ministerio de Educación y Ciencia for a Ramón y Cajal contract and A. M. N for a predoctoral research grant from CSIC (I3P program). We thank Mrs. M. C. Jimenez de Haro for SEM images of the polyethylene samples and Mr. A. Giacometti Schieroni for carrying out the GPC analysis.

[1] a) B. L. Small, M. Brookhart, A. M. A. Bennett, *J. Am. Chem. Soc.* **1998**, *120*, 4049–4050; b) G. J. P. Britovsek, V. C. Gibson, B. S. Kimberley, P. J. Maddox, S. J. Mc Tavish, G. A. Solan, A. J. P. White, D. J. Williams, *Chem. Commun.* **1998**, 849–850.

[2] a) V. C. Gibson, C. Redshaw, G. A. Sola, *Chem. Rev.* **2007**, *107*, 1745–1776; b) C. Bianchini, G. Giambastiani, I. Guerrero Rios, G. Mantovani, A. Meli, A. M. Segarra, *Coord. Chem. Rev.* **2007**, *250*, 1391–1418.

[3] J. R. Severn, J. C. Chadwick, R. Duchateau, N. Friederichs, *Chem. Rev.* **2005**, *105*, 4073–4147.

[4] See for exsample: a) V. C. Gibson, S. K. Spitzmesser, *Chem. Rev.* **2003**, *103*, 283–315; b) B. L. Small, M. Brookhart, *Macromolecules* **1999**, *32*, 2120–2130; c) G. J. P. Britovsek, M. Bruce, V. C. Gibson, B. S. Kimberley, P. J. Maddox, S. Mastroianni, S. J. McTavish, C. Redshaw, G. A. Solan, S. Strömberg, A. J. P. White, D. J. Williams, *J. Am. Chem. Soc.* **1999**, *121*, 8728–8740; d) Y. Chen, C. Qian, J. Sun, *Organometallics* **2003**, *22*, 1231–1321; e) K. P. Tellmann, V. C. Gibson, A. J. P. White, D. J. Williams, *Organometallics* **2005**, *24*, 280–286; f) A. S. Ionkin, W. J. Marshall, D. J. Adelman, B. Bobik Fones, B. M. Fish, M. F. Schiffhauer, *Organometallics* **2006**, *25*, 2978–2992.

[5] a) C. Amort, M. Malaun, A. Krajete, H. Kopacka, K. Wurst, M. Christ, D. Lilge, M. O. Kristen, B. Bildstein, *Appl. Organomet. Chem.* **2002**, *16*, 506–516; b) C. Bianchini, G. Giambastiani, G. Mantovani, A. Meli, D. Mimeau, *J. Organomet. Chem.* **2004**, *689*, 1356–1361; c) G. J. P. Britovsek, V. C. Gibson, B. S. Kimberley, S. Mastroianni, C. Redshaw, G. A. Solan, A. J. P. White, D. J. Williams, *J. Chem. Soc., Dalton Trans.* **2001**, 1639–1644; d) G. A. Luinstra, J. Queisser, B. Bildstein, H.-H. Görtz, C. Amort, M. Malun, A. Krajete, G. Werne, M. O. Kristen, N. Huber, C. Genert, in *Late Transition Metal Polymerization Catalysts* (Eds.: B. Rieger, L. Saunders Baugh, S. Kacker, S. Strigler), Wiley-VCH, Weinheim, Germany, **2003**.

[6] a) R. Schmidt, M. B. Welch, S. J. Palackal, H. G. Alt, *J. Mol. Catal. A* **2002**, *179*, 155–173; b) S. McTavish, G. J. P. Britovsek, T. M. Smit, V. C. Gibson, A. J. P. White, D. J. Williams, *J. Mol. Catal. A* **2007**, *261*, 293–300; c) A. M. Archer, M. W. Bouwkamp, M.-P. Cortez, E. Lobkovsky, P. J. Chirik, *Organometallics* **2006**, *25*, 4269–4278.

[7] T. M. Smit, A. K. Tomov, V. C. Gibson, A. J. P. White, D. J. Williams, *Inorg. Chem.* **2004**, *43*, 6511–6512.

[8] G. J. P. Britovsek, V. C. Gibson, O. D. Hoarau, S. K. Spitzmesser, A. J. P. White, D. J. Williams, *Inorg. Chem.* **2003**, *42*, 3454–3465.

[9] M. Seitz, W. Milius, H. G. Alt, *J. Mol. Catal. A* **2007**, *261*, 246–253.

[10] F. Pelascini, M. Wesolek, F. Peruch, P. J. Lutz, *Eur. J. Inorg. Chem.* **2006**, 4309–4316.

[11] a) S. Milione, C. Cavallo, C. Tedesco, A. Grassi, *J. Chem. Soc., Dalton Trans.* **2002**, 1839–1846; b) A. M. A. Bennett, World Patent, WO9827124, **1998**; c) P. Barbaro, C. Bianchini, G. Giambastiani, I. Guerrero Rios, A. Meli, W. Oberhauser, A. M. Segarra, L. Sorace, A. Toti, *Organometallics* **2007**, *26*, 4639–4651; d) C. Bianchini, G. Giambastiani, I. Guerrero Rios, A. Meli, W. Oberhauser, L. Sorace, A. Toti, *Organometallics* **2007**, *26*, 5066.

[12] J. Cámpora, C. M. Pérez, A. Rodríguez-Delgado, A. Marcos Naz, P. Palma, E. Álvarez, *Organometallics* **2007**, *26*, 1104–1107.
[13] G. J. P. Britovsek, V. C. Gibson, S. K. Spitzmesser, K. P. Tellmann, A. J. P. White, D. J. Williams, *J. Chem. Soc., Dalton Trans.* **2002**, 1159–1171.
[14] H. G. Alt, *Dalton Trans.* **2005**, 3271–3276.
[15] F. A. R. Kaul, G. T. Puchta, H. Schneider, F. Bielert, D. Mihalios, W. A. Herrmann, *Organometallics* **2002**, *21*, 74–82.
[16] G. Jin, D. Zhang, *J. Polym. Sci. Part A* **2004**, *42*, 1018–1024.
[17] B. L. Small, A. J. Marcucci, *Organometallics* **2001**, *20*, 5738–5744.
[18] C. Görl, H. G. Alt, *J. Mol. Catal. A* **2007**, *273*, 118–132.
[19] *Apex 2*, version 2.1, Bruker AXS Inc., Madison, Wisconsin, USA, **2004**.
[20] *SAINT* and *SADABS*, Bruker AXS Inc., Madison, Wisconsin, USA, **2001**.
[21] *SIR2002*: The Program: M. C. Burla, M. Camalli, B. Carrozzini, G. L. Cascarano, C. Giacovazzo, G. Polidori, R. Spagna, *J. Appl. Crystallogr.* **2003**, *36*, 1103.
[22] G. M. Sheldrick, *SHELXL97*, University of Göttingen, Germany, **1997**.

Received: November 12, 2007
Published Online: February 22, 2008

